



Contribution

# Filling and Emptying of Gravure Cells - A CFD Analysis -

J. M. Brethour  
Flow Science, Inc.

## 1. Introduction

Gravure roll coating is commonly used where low coat weights are to be applied at high speed. In such situations, roll coating can be problematic because the coat weight is sensitive to the intricate balance of viscous, capillary and inertial forces within the roll gap. Slight changes in speed or roll gap can drastically affect the final coating thickness when the desired coat weight is small. With gravure rolls, much of the coating fluid is contained within the gravure cells, which is a fixed volume for each roll. Therefore, the final coat weight is less a function of less-controlled parameters (fluid viscosity, surface tension and roll speed) and more a function of the cell geometry, which can be finely controlled for each application.

In gravure roll coating, the key to understanding how the cells fill and empty is to study the processes occurring within individual cells. This is very difficult to do experimentally because of the minute size of the gravure cells: they are typically less than  $100\mu\text{m}$  across. Also, the speed at which a gravure roll rotates (typically

visualization virtually impossible. Therefore, little study has been done of the cell filling and emptying of individual gravure cells. Schwartz<sup>1)</sup> presented a numerical model of the gravure cell withdrawal process; this work did not include effects of entrapped air within the cell or the effects of inertia.

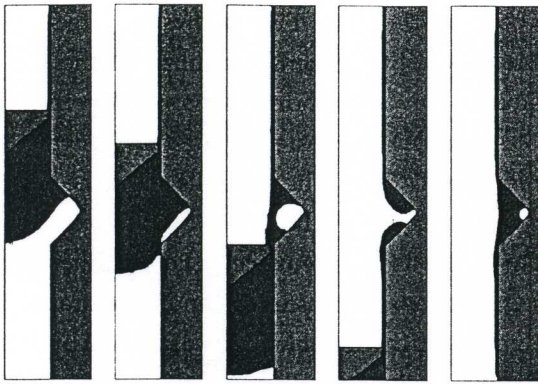
In this paper the numerical fluid flow model is based on a finite-control-volume technique. This method does not impose specific flow values at any point (such as along contact lines and no-slip boundaries), but rather keeps track of the mass and momentum in each control volume element. The locations of fluid interfaces are tracked by a volume-of-fluid (VOF) method in which the fluid fraction within each mesh cell is tracked and stored. Using the fluid fractions of neighboring cells, free surfaces can be located, and surface slopes and curvatures can be computed<sup>2)</sup>. Newtonian fluid properties were used for all simulations presented in this paper.

At contact lines, an additional force describing the adhesion between the solid and the liquid is added along with the dynamic

conservation. This adhesion force is assumed to arise from molecular interactions between the solid and liquid. The interaction is characterized by the static contact angle because the molecular processes that cause the adhesion force act at a space and time scale far smaller and faster than those of the flow process. Therefore, the wall adhesion force is computed from the cosine of the static contact angle and the interfacial tension between the air and the liquid<sup>3)</sup>.

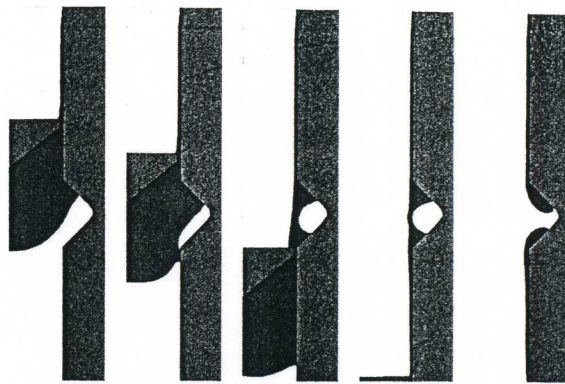
In the gravure coating process, air can become trapped. In this model, the trapped air behaves isentropically with PV1.4 held constant to control the pressure-volume relation for regions with trapped gas. There is no transfer of energy or mass between the fluid and the gas bubble. In open gas regions, the gas pressure is fixed to be atmospheric.

All of the simulations presented here were computed using this combined control-volume-VOF method as it has been implemented in the commercial software package FLOW-3D<sup>®</sup> developed by Flow Science, Inc., Santa Fe, New Mexico, USA<sup>4)</sup>.



\* The static contact of the fluid on the gravure roll is  $30^\circ$ .  
\* The elapsed time here is  $170\mu\text{s}$ .

**Fig.1** Two-dimensional slice down the centreline of a three-dimensional simulation of gravure cell filling at  $2\text{m/s}$ .



\* The elapsed time is  $196\mu\text{s}$ .

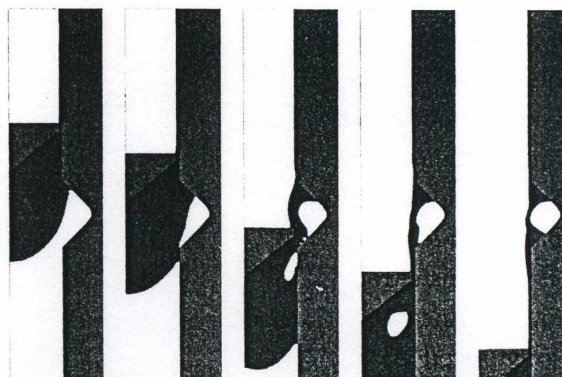
**Fig.2** Similar case as in Fig.1 but static contact angle to gravure roll is now  $60^\circ$ .

## 2. Filling of a Gravure Cell

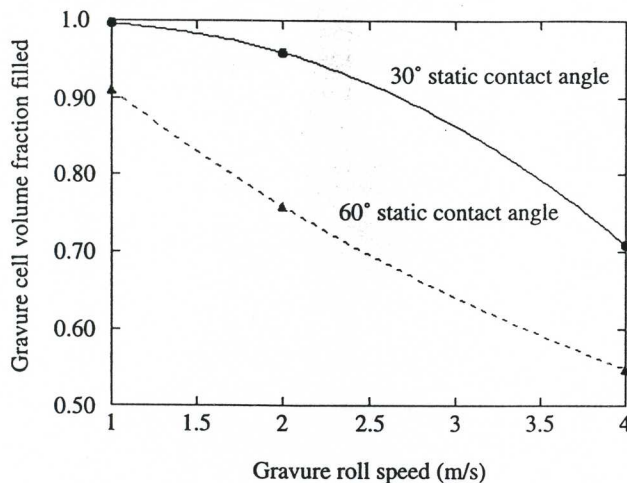
Within the grid of finite control volume elements, one gravure cell was created by blocking off to flow elements located within solid regions, and those elements partly blocked by the solid are partially blocked to flow by manipulating the area fractions open to flow in each of the three Cartesian directions adjacent to each element. The gravure cell for all simulations is pyramidal in shape, with width and length each  $80\mu\text{m}$ , and a maximum depth of  $40\mu\text{m}$ . Also created within the mesh is a rigid solid blade, which translates downward in the model. The minimum gap between the blade and the gravure roll surface is  $3.5\mu\text{m}$ . The fluid's viscosity is  $10\text{cpoise}$ , its density is  $1\text{g/cm}^3$  and the air-liquid surface tension is  $60\text{mN/m}$ . The static contact angle between the liquid and the blade is  $30^\circ$  for all cases. The static contact angle between the liquid and the gravure roll and the roll speed vary

Fig.1 shows the time evolution of the cell filling process of a two-dimensional slice down the centre of the gravure cell; the static contact angle with the gravure roll is  $30^\circ$  and the web speed is  $2\text{m/s}$ . The advancing contact line at the front edge of the liquid bead moves into the gravure cell, but before the contact line is able to advance up the opposing side of the cell the liquid bead makes contact with the downstream lip of the cell, trapping an air bubble inside the cell. After the blade has passed over the cell, the liquid overlying the bubble thins due to the superambient

pressure within the bubble and the bulge it causes on the outer liquid interface. The bubble ruptures, leaving a smaller bubble behind, and the resulting final fluid interface has a dimple over the gravure cell. This is similar to what was postulated by Schwartz<sup>1)</sup>. Fig.2 shows the same case but with the static contact angle to the gravure roll raised to  $60^\circ$ . In this case, the volume of air trapped in the gravure cell is larger because the advancing contact line moves more slowly than the  $30^\circ$  case. The result is a deeper dimple in the final profile. Fig.3 is a plot of the volume



\* The elapsed time is  $67\mu\text{s}$ .



**Fig.4** Plot of fraction of cell volume filled as a function of gravure roll speed for various static contact angles.

fraction filled as a function of gravure roll speed for various static contact angles. Greatest fill fractions are obtained with low roll speed and low static contact angles. Low roll speeds allow the advancing contact to enter farther into the cell before the air is trapped by the liquid bead being pushed by the blade. Low contact angles result in faster advance of the contact line.

## 3. Emptying of a Gravure Cell

Again, a gravure cell of the same dimensions was created within the grid of finite control volumes, but instead of a translating blade, the pulling away of the substrate from the surface of the gravure roll was modelled by creating a solid block that translates linearly away from the roll. This motion is adequate to describe the separation because at such small scales the transfer roll would appear to move linearly away from the gravure roll. Also, the fluid initially in the cell was presumed from observing the

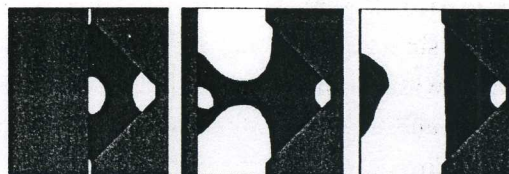
simulations. A bubble was placed in the bottom of the cell and the dimple at the cell's free surface becomes a bubble adjacent to the transfer roll. Fig.4 shows the case where the transfer roll is pulling away at 0.5m/s and the static contact angle with all surfaces is 30°. Fig.5 shows the same case except that the static contact angle of the liquid to the gravure cell is

60°. Fig.6 shows the three-dimensional image of the withdrawal process 75 $\mu$ s after the transfer roll first pulls away.

These results show the necking of the liquid as it pulls away from the gravure cells; liquid adheres to the transfer roll and the entrapped bubble that was caused by the dimple in the fluid surface over the gravure cell ruptures through, leaving behind a dot on the transfer roll. In the sample results presented here, the volume transferred is far smaller than the volume initially present in the gravure cell. Also, higher speeds and/or higher contact angles cause the volume of fluid adhering to the transfer roll to fall.

## 4. Summary

A numerical simulation method of the filling and emptying of individual gravure cells has been



\* The transfer roll surface (block at left) is moving away from the gravure roll at 0.5m/s.

\* The static contact of the fluid with all surfaces is 30°.

**Fig.5** Emptying of gravure cell (same cell dimensions as filling case); a two-dimensional slice down the centerline of the cell is shown.

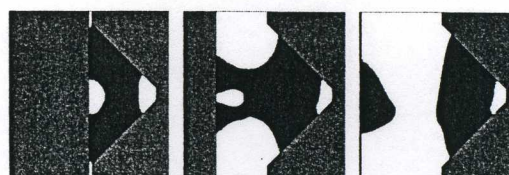


**Fig.6** Same case as Fig.4 but the static contact angle to



\* The case shown here is the same as in Fig.4.

\* The transfer roll surface is removed from this picture for clarity.

Fig.7 Three-dimensional image of gravure cell withdrawal process.

performed for a variety of sample cases showing the effect of the static contact angle (with the gravure roll surface) and the speed of roll rotation. The advantage of this method is the ability to study the movement of free surfaces into the cell on any desired time scale with

any desired cell geometry with any desired fluid. This is not possible with existing fluid visualization techniques.

The results demonstrate how roll speed and the static contact angle affect the movement of fluid into the gravure cell. Lower static contact angles and low speeds are most conducive to ensuring maximum fill or emptying of the cells because the advancing contact line is able to move into the cell before the liquid bead traps air inside. Because the model approach described in this paper exists in a commercial software package<sup>4)</sup>, it is available for immediate application to the investigation of quality issues associated with many types of coating applications.

Finally, this article was presented

at the 4th European Coating Symposium 2001, Oct. 1~4 2001, Brussels, Belgium.

<Reference>

- 1) Schwartz, L.W., Moussalli, P., Campbell, P. and Eley, R. R., Numerical modelling of liquid withdrawal from gravure cavities in coating operations, *Trans IChemE*, 76(A), 22~28 (1998)
- 2) Hirt, C.W. and Chen, K.S., Simulation of slide-coating flows using a fixed grid and a volume of fluid front-tracking technique, *Proc. 8th International Symposium on Coating Science and Technology*, New Orleans (1996)
- 3) Young, T., An essay on the cohesion of fluids, *Phil. Trans. Royal Soc. (London)*, 95, 65 (1805)
- 4) FLOW-3D® User's Manual, Flow Science, Inc. report FSI-00-1 (2000), [www.flow3d.com](http://www.flow3d.com).

## FOUNDATION OF NEW FIRM

EarthShell Corp. announced that it has handed over its Goleta manufacturing operations to Green Earth Packaging Inc. and will collect royalties as part of the deal.

Green Earth assumed responsibility for all production of biodegradable EarthShell plates and bowls at the 55,000-square-foot facility on Fairview Avenue. The company will be the first manufacturer to pay royalties to EarthShell for products sold.

EarthShell food packaging, which includes clamshells and sandwich wraps, is made primarily from limestone and potato starch. When the products are crushed or broken, it begins to biodegrade once it's exposed to moisture or when composted.

EarthShell bills it self as a technology firm focused on developing biodegradable food packaging. It has never intended to manufacture the products beyond the research and testing phase, and instead licenses the technology to operating partners (manufacturers) that handle production.

Green Earth Packaging and its sister company, Green Packaging, both subsidiaries of Malaysian manufacturing group Dominance Inc., became EarthShell licensees in December 2001.

And then, EarthShell announced that the two licensees would invest a minimum of \$30 million to fund the building of a new manufacturing facility that was originally expected to begin commercial shipments during the first quarter of 2002.

More than a year later, Green Earth is in the process of finding a manufacturing location in the United States, and there is strong interest in building the plant in Texas, said Vice Truant, president of EarthShell, and the new facility is expected to be fully operational before the lease at the Goleta plant expires in May 2003, said Mr. Truant.

Green Earth and Green Packaging have set a target of producing more than one billion units of EarthShell products annually, with market sales estimated at more than 50 million, at the yet-to-be-built facility.

As of its second quarter ended in June, EarthShell has accumulated net losses of \$274 million since inception in 1992. EarthShell has yet to show any profits and expects further losses until its manufacturing partners begin to produce and sell mass quantities of its products.

For more information contact: EarthShell Corporation; Tel: +1-410-847-9420; URL: <http://www.EarthShell.com>